THE JOURNAL OF PHYSICAL CHEMISTRY Letters

LETTER

pubs.acs.org/JPCL

Topologically Mismatched Pinning of Scroll Waves

Sumana Dutta and Oliver Steinbock*

Department of Chemistry and Biochemistry, Florida State University, Tallahassee, Florida 32306-4390, United States

Web-Enhanced

ABSTRACT: Three-dimensional scroll waves in excitable reaction−diffusion systems rotate around one-dimensional phase singularities. Although these filaments are dynamic objects, their motion can be arrested if pinned to unexcitable obstacles. We study this vortex pinning for a case in which the topology of the initial filament (circular loop) differs from the topology of the obstacle (double torus). In experiments with the Belousov−Zhabotinsky reaction and numerical simulations, we show that pinning is possible and that it induces periodic rotation patterns. Continuous rotation extends around either one or both halves of the double torus. The latter case is doubly degenerate because waves can move through the two holes in the same or opposite directions. Opposite rotation is organized by a two-armed vortex segment that emits waves at a period approximately two-times larger than the other pinned vortex states.

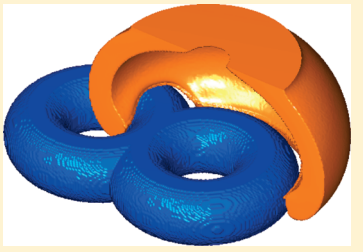

SECTION: Macromolecules, Soft Matter

Propagating excitation waves exist in a variety of chemical and biological systems. These concentration waves have characteristic speeds and amplitudes, which result from the diffusion-mediated spreading of an autocatalytic reaction zone.[1] Classic examples include the Belousov−Zhabotinsky (BZ) reaction,[2] uncatalyzed bromate oscillators,[3] the chlorite−iodide−malonic acid reaction,[4] and the CO oxidation on platinum surfaces.[5] Investigations of these chemical nonequilibrium phenomena continue to impact research in systems biology and medicine. For instance, calcium waves in cells and traveling action potentials in neuronal and cardiac tissues have very similar characteristics and dependencies as waves in synthetic, chemical systems.[6−8]

In spatially two-dimensional media, excitation waves can form rotating vortices.[9,10] Their wave fronts (i.e., the autocatalytically active region) trace constant-pitch, Archimedean spirals. The (interior) end of the front is called the spiral tip. Its dynamics has been studied in great detail and can be as simple as rotation around a closed circular trajectory or as complex as quasiperiodic and chaotic motion.[10] In the former case, the circular orbit surrounds a region known as the spiral core. Within this disk-shaped core, concentration changes have the same periodicity as those in the main pattern, but their amplitude is much smaller. The center of the core has a phase singularity where the phase of oscillation is undefined.

Rotating waves exist also in three-dimensional systems.[11] These are scroll waves that importantly here cannot rotate around points but must move around one-dimensional curves known as filaments. The simplest scroll wave is constructed by stacking up identical two-dimensional spirals in the normal direction. A continuous rotation of the spirals during construction creates a geometrical twist. Filaments can also deviate from straight lines, which induces motion with speeds proportional to the local filament curvature.[11−13] Moreover, filaments cannot terminate within the system but only at (external and internal) system boundaries (for the only known exception, see ref 2). Alternatively, they can form closed loops and knots,[14] but they cannot branch and must obey certain topological constraints.[15]

Recent experiments with the autocatalytic BZ reaction have demonstrated the pinning of scroll waves to nonreactive, impenetrable heterogeneities such as small spherical beads and thin torus-shaped obstacles.[16,17] In the latter case, scroll waves rotate strictly around the inert torus, thus preventing the curvature-induced collapse that is characteristic for the unpinned vortex.[17] Spherical obstacles fail to prevent the collapse but increase the lifetime of the vortex ring by 25% regardless of the size of the initial filament loop.[18] If the circumference of the pinning obstacle is larger than the length of the free tip orbit, the rotation period is increased. This effect generates twist, which is limited by the (smoothing) reaction−diffusion processes according to a nonlinear diffusion equation (the Burgers equation).[11,19]

Despite recent progress toward a better understanding of scroll wave pinning, this interesting phenomenon is widely understudied. Key questions that remain unanswered concern filament capture and unpinning, dynamics in highly heterogeneous (random and ordered) systems, and applications in the life sciences. For instance, scroll waves of electric activity have been linked to tachycardia and ventricular fibrillation in the human heart.[7,20] There is growing evidence that these three-dimensional excitation vortices can be influenced or pinned by insulating tissue regions such as scar tissue caused by heart attacks.[21] From a more fundamental point of view, there are also intriguing challenges regarding the exploration of frustrated vortex states

Received: March 8, 2011
Accepted: April 5, 2011
Published: April 12, 2011

ACS Publications © 2011 American Chemical Society

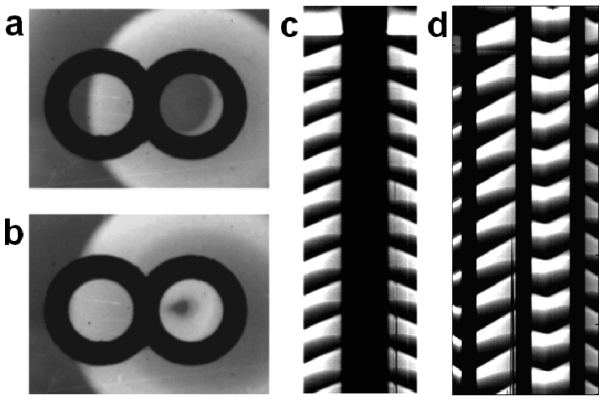

Figure 1. W A single scroll wave pinned to an inert double torus in the three-dimensional BZ reaction. The transmission images (a,b) show the top view of the pinned oxidation wave (bright regions). Scroll wave rotation occurs around the right subtorus. The time−space plots (c,d) are constructed from intensity profiles that cut the image data centrally in vertical (c) and horizontal (d) directions. In both plots, time evolves in a downward direction covering 92.7 min. The field of view in (a,b) is 1.9×1.4 cm^2. Frame (a) is recorded 100 s prior to frame (b). A movie of this experiment is available.

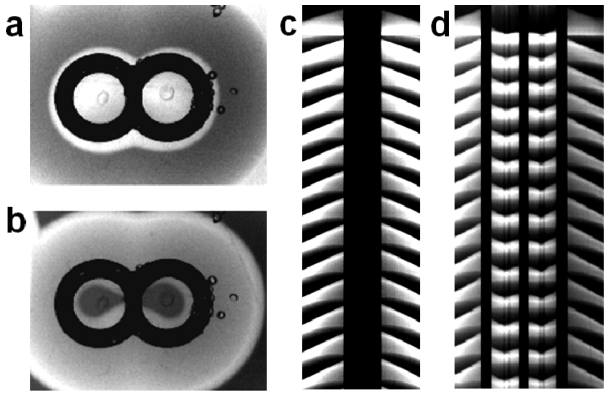

Figure 2. W A pair of scroll waves pinned to an inert double torus in the three-dimensional BZ reaction. The transmission images (a,b) show the top view of the pinned oxidation wave (bright regions). Scroll wave rotation involves both subtori. The time−space plots (c,d) are constructed from intensity profiles that cut the image data centrally in vertical (c) and horizontal (d) directions. In both plots, time evolves in a downward direction covering 100 min. The field of view in (a,b) is 2.1×1.6 cm^2. Frame (a) is recorded 210 s prior to frame (b). A movie of this experiment is available.

in which the topology of the pinning heterogeneity differs from the topology of the filament. In this Letter, we investigate a simple example of the latter situation, namely, the pinning of filament loops to a simple genus-2 object.

Our experimental system is the excitable BZ reaction, which involves the oxidation of malonic acid by bromate in an acidic solution. BZ waves are driven by the diffusion and autocatalytic production of bromous acid. During the autocatalysis, ferroin is oxidized and changes color, which allows us to detect wave patterns by spatially and temporally resolved photometry. Pattern formation in this closed system occurs for several hours, but substantial changes in the wave velocity and period are observed after 6 h. The setup, the preparation of the reaction system, the initiation of a vortex ring, and the pinning procedure are described in the Experimental and Numerical Methods section. The pinning obstacle is made of a fluoropolymer elastomer and has the shape of a double torus. The unbranched ring segments have a thickness of 1.5 mm, and the holes of the double torus have a diameter of 4.0 mm. In the homogeneous system, the pattern wavelength of the scroll waves is 5.5 mm.

Visual inspection of a long image sequence clearly reveals a periodic motion in which wave fronts of circular appearance are emitted from the right half of the double torus. This pattern also involves inward-moving waves within the right torus. In the left half of the double torus, however, waves seem to propagate across the entire opening in a leftward direction. The period of these events is 520 s.

The latter description is quantified in the time−space plots in Figure 1c,d. The plots result from one-dimensional intensity profiles that we obtain from images similar to those in Figures 1a,b. With respect to the orientation of those images, the profiles are extracted along constant lines cutting though the middle of the double torus in vertical (Figure 1c) and horizontal directions (Figure 1d). In the following, we will refer to these lines in terms of the coordinates x_1 and x_2, respectively. In both plots, time evolves in a downward direction, while the horizontal axis is the space axis x_i. Figure 1c shows periodic wave emission in the $+x_1$ and $-x_1$ directions. This wave emission is phase-synchronized because the image data are symmetric

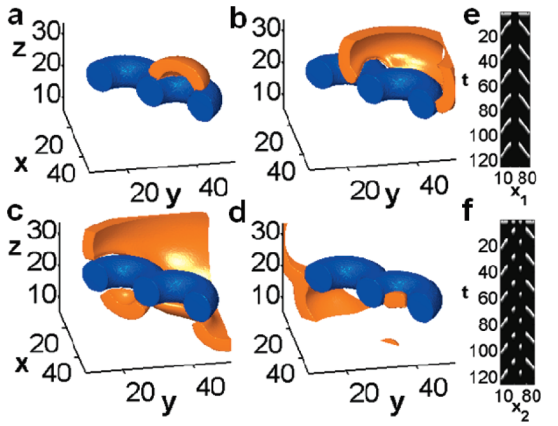

Figure 3. Numerical simulation of a single scroll ring pinned to a double torus. In the image sequence (a−d) excited regions ($v \geq 0.4$) are solid yellow; the pinning double torus is solid blue. Data from the anterior half of the system is omitted, and the computed volume is also cropped along all boundaries. The time−space plots in (e) and (f) summarize the wave motion in the central plane of the medium ($z = 20$). They are constructed from wave profiles along lines cutting the double torus at its thinnest (e) and widest point (f).

with respect to the (horizontal) x_2 axis. Notice that the black area is caused by the double torus. The time−space plot in Figure 1d cuts the anchor three times. Again, the vortex emits waves in an outward direction, although some external waves affect the structure during the very early and late stages. More importantly, one can discern a steady leftward motion in the left hole region and a bidirectional, inward motion within the right hole. The latter causes V-shaped bands with tips (i.e., the collision points) slightly shifted toward the left.

We also attempted to initiate scroll wave rotation around both of the connected tori. These experiments require the initiation of two half-spherical waves, each capping one individual torus. Such an experiment is illustrated in Figure 2. Like in Figure 1, we show two snapshots and two time−space plots. Again we observe a periodic pattern, but the period (420 s) is 19% lower than that in

dx.doi.org/10.1021/jz2003183 |J. Phys. Chem. Lett. 2011, 2, 945–949

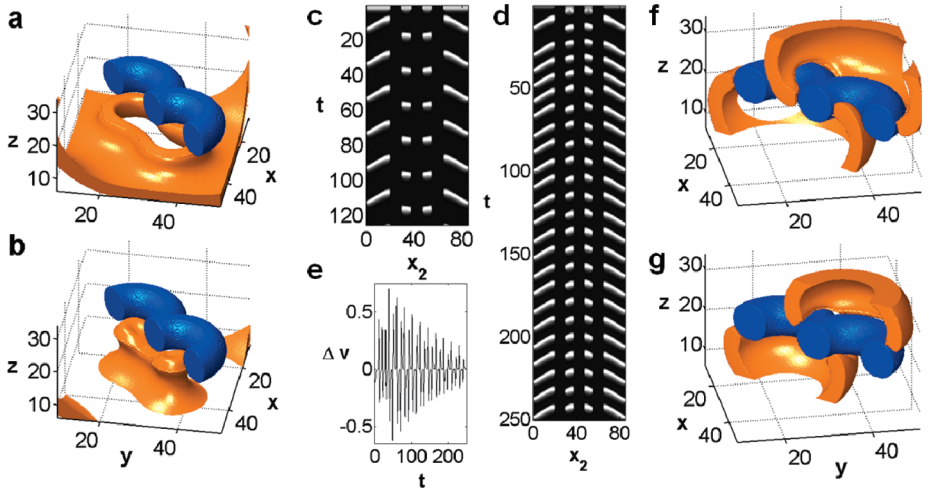

Figure 4. Ⓦ Numerical simulation of scroll ring pairs pinned to a double torus. In (a−c), both vortices traverse the double torus holes in the upward direction, while in (d−g), the left vortex passes through the left hole in a downward direction. As in Figure 3, the wave fields (a,b,f,g) are rendered in solid yellow, while the pinning obstacle is blue. The images in (a,b) show the entire wave structure but only the posterior half of the obstacle. Both time−space plots (c,d) are obtained along the line of widest extension of the double torus. The graph in (e) shows the temporal evolution of the difference in v values at the two hole centers of the double torus. A movie of the simulation shown in (f,g) is available.

Figure 1. Notice that the images (Figure 2a,b) are essentially symmetric with respect to the x_1 and x_2 axes. Furthermore, the time−space plot in Figure 2d reveals V-shaped bands in both hole regions. Symmetry with respect to the x_2 axis was frequently lost if we employed double tori with larger holes (data not shown). The origin of this phenomenon is unclear.

Our experiments provide unambiguous evidence that scroll rings can pin to an inert double torus. They also demonstrate the existence of two, strikingly different, pinned vortex states. However, due to the limitations of our detection method, they cannot provide detailed insights into the full three-dimensional dynamics. We therefore performed numerical simulations based on a reaction−diffusion model (see Experimental and Numerical Methods section for details).

Figure 3a−d shows a sequence of three-dimensional concentration fields in which the excitation vortex is visualized as a solid (yellow) area while the pinning double torus is plotted in blue. The anterior half of the system is excluded to yield an unobstructed view of the pattern. Anterior and posterior halves are symmetric with respect to the cutting plane.

The situation in Figure 3a is similar to the initial condition in the experiment shown in Figure 1. A small wave cap is located on the right half of the pinning double torus. This cap expands and begins to rotate around its subtorus (Figure 3b). However, the motion is blocked in the X-shaped region where the two tori meet. The branching torus punches a hole in the leading edge of the rotating vortex. Between the branching points (i.e., in the mid region of the double torus), the rotation proceeds nearly unperturbed and extends through the left hole to eventually cause a collision of the wave with the distant end of the left torus (Figure 3c). This collision splits the wavefront temporally before rejoining at the outermost, left regions of the double torus (Figure 3d). During the latter stage, the rotation around the right torus has created a small wave segment filling the hole of that torus. This situation leads directly back into the situation shown in Figure 3a, thus closing the rotation cycle.

Figure 3e,f shows the corresponding time−space plots. In contrast to their experimental counterparts, they are generated from actual variable profiles in the central plane of the system ($z = 20$). They qualitatively agree well with the data in Figure 1c, d, but the V-shaped features from the experimental plots are nearly absent. We believe that this minor discrepancy is caused by the comparably smaller hole size in the simulations.

The case of two scroll rings pinned to a double torus is illustrated in Figure 4a−c. The frames (a,b) show the entire wave field but only the posterior half of the pinning obstacle. Notice that the branching points of the double torus, and hence the underlying topological mismatch, also affect this simpler structure. Here, they cause a slight twisting of the vortices, which is due to a longer path around the branching points. The buildup of this delay to large twist patterns is limited by the reaction−diffusion characteristics of the system.[18,19] Twist can also be discerned in the time−space plot (Figure 4c) by the slight tilt of the wave bands in both hole regions. Notice that this branching-induced delay is also discernible in the experiment shown in Figure 2b.

The pinning of two vortices to a double torus involves an interesting degeneracy. So far, all scroll wave pairs had a uniform sense of rotation, that is, they traversed the holes of the double torus in the same direction. However, it is also possible to pin vortices of opposite rotation sense. This case is shown in Figure 4d−g. The three-dimensional wave fields (f,g) reveal the presence of a two-armed scroll wave rotating (counter-clockwise) around the central junction segment of the double torus. The remainder of the anchor pins single-armed scroll waves. This complex pattern is dynamically stable, as shown by the time−space plot data in Figure 4d. Notice that the two-armed vortex is the primary pacemaker of the pattern. Accordingly, the frequency of wave emission is approximately two (1.8) times larger than the frequency of the strictly one-armed rotors (Figures 3 and 4a−c). Further inspections of the time−space plot in Figure 4d reveal long-lived phase variations between the two vortex components, in which the individual periods alternate between above and below average values. We document this minor transient effect in Figure 4e, which plots the difference between the v values in the two torus centers. Notice that this measure equals 0 for perfectly synchronized vortices.

The rotation patterns around the double torus involve surprisingly complex dynamics of the contact line between the wave

dx.doi.org/10.1021/jz2003183 |J. Phys. Chem. Lett. 2011, 2, 945–949

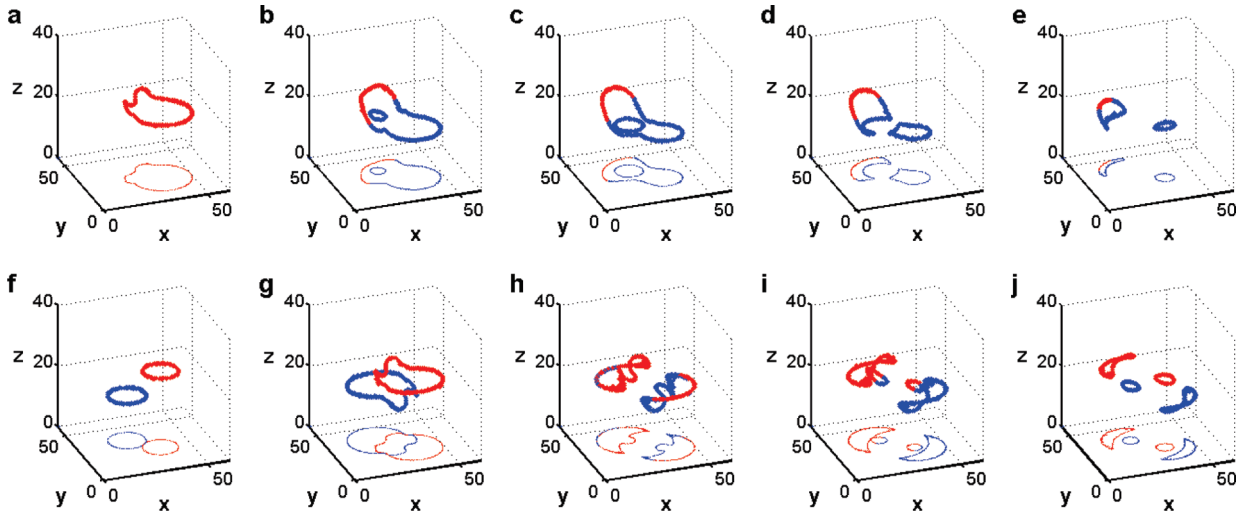

Figure 5. Ⓦ Filament evolution in simulations of pinned scroll wave rotation. The sequence (a−e) shows a single scroll wave (same as that in Figure 3), while (f−j) describes a pair of scroll waves that penetrates the holes of the double torus in opposite directions (the case shown in Figure 4e,f). Red and blue curve segments indicate points above and below the central obstacle plane ($z = 20$). The filaments are also projected into the bottom plane ($z = 0$). Time intervals between neighboring frames are 3.3, 5.8, 6.6, 8.8 (a−e) and 4.0, 5.3, 6.0, 7.3 (f−j). Movies illustrating the simulated filament dynamics in (a−e) with and without wave fields, a movie for (f−j), and also a movie for the case shown in Figure 4a−c are available.

structure and the obstacle. This line is closely related to the filament, although some of its parts are not performing a continuous orbiting motion. Figure 5a−e shows a sequence of snapshots for the case illustrated in Figure 3. In frame (a), the contact line is a single, continuous loop located on top of the double torus. The deformations from a simple circle are due to the branching structure of the double torus. Frame (b) shows an additional loop that is split off when the wave arm rotating around the obstacle's X-shaped midsection collides with the distant half of the double torus (see Figure 3c). The split-off loop moves downward and then collides with the main loop at two different locations (Figure 5c,d). In these simultaneous collisions, the curves reconnect, and two new loops are formed. The posterior one shrinks and annihilates, while the anterior loop travels in an upward direction through the hole to complete the cycle (Figure 5e). The second row (Figure 5f−j) illustrates the filament dynamics for the case of a vortex passing through the holes in opposite directions (i.e., the case in Figure 4f,g). The dynamics share certain similarities with the earlier scenario, but at all times, either two or four filament loops are present.

In conclusion, we have shown that scroll waves can pin to topologically mismatched anchors, and we identified three qualitatively different solutions for the case of a double torus. Our results provide the starting point for more systematic investigations of rotating three-dimensional chemical waves in media with high-density heterogeneities where branching points of the inert obstacles will be frequent. Moreover, we believe that our study could lead to a better understanding of tachycardia and ventricular fibrillation in scarred heart tissue.

EXPERIMENTAL AND NUMERICAL METHODS

The initial concentrations of the BZ system are [malonic acid] = 0.04 M, [BrO_3^-] = 0.04 M, [H_2SO_4] = 0.016 M, and [ferroin] = 0.5 mM. We prepare all solutions in nanopure water (18 MΩ cm). Experiments are carried out at room temperature. The reaction system is illuminated with white light. A charge-coupled device camera (COHU) equipped with a dichroic blue filter monitors absorption changes. The BZ system consists of two layers contained in a Petri dish. The lower layer is a BZ agarose gel (0.8 w/v%; thickness 4.8 mm), while the upper layer (thickness 3.2 mm) is a liquid BZ solution. The camera records images in the plane of the layer interface.

The double-torus-shaped obstacle is produced by joining two O-rings (Viton, ORI Co.) with Devcon HP250 polymer adhesive glue. To create a smooth connection, both O-rings are locally cut at half-thickness, so that the width of the X-shape junction is very close to the width of the individual rings. After thorough rinsing, the pinning obstacle is placed onto the gel surface shortly after transfer of the BZ agarose solution into the Petri dish and gently pressed into the forming gel.

Scroll waves are initiated by creating half-spherical waves that are centered over a given hole of the double torus and also cap the respective torus. For this purpose, a silver wire is temporarily inserted into the reaction system, and its tip is carefully positioned at the hole's center. The silver wire decreases the local concentration of the inhibitor species bromide and, thus, triggers a wavefront best described by a spherically capped cylinder. Once this front reaches the double torus, the liquid BZ layer is mixed and homogenized by shaking of the sample. After fluid motion ceases, all chemical waves in this layer have vanished. In the lower gel layer, however, a half-spherical wave remains. The rim of this bowl-shaped wave is connected to one torus-half of the double torus and commences the desired rotation around the obstacle.

Our simulations are based on the Barkley model, which is frequently used to describe excitable reaction−diffusion systems.[22] It involves two variables u and v that can be loosely associated with the concentrations of bromous acid and the oxidized form of ferroin. The variables obey

$$\partial u/\partial t = D_u \nabla^2 u + \varepsilon^{-1} u(1-u)[(u-(v+b)/a] \quad (1a)$$

$$\partial v/\partial t = D_v \nabla^2 v + u - v \quad (1b)$$

where the system parameters ε, a, and b are kept constant at 0.02, 1.1, and 0.18, respectively. The diffusion constants are $D_u = D_v = 1$. This set of parameters describes a system in which spiral

dx.doi.org/10.1021/jz2003183 |J. Phys. Chem. Lett. 2011, 2, 945–949

and scroll waves undergo rigid rotation. Equations 1a and 1b are integrated using explicit Euler integration, a seven-point stencil for the Laplacian, a three-dimensional lattice measuring 300 × 300 × 200 grid points, and Neumann boundaries. The grid spacing and the integration time step are kept constant at 0.2 and 0.006, respectively. The pinning double torus is modeled as a region in which u and v equal 0. The individual tori are described by a disk of diameter 8.8 space units rotating around a circle of radius 17.6 space units. The tori overlap fully at the central junction. The filament is computed from the intersection of the waves' $u = 0.5$ and $v = a/2 - b$ surfaces using a marching-cube algorithm.[23]

Web Enhanced Feature. Movies of various experiments and simulations.

AUTHOR INFORMATION

Corresponding Author

*E-mail: steinbck@chem.fsu.edu.

ACKNOWLEDGMENT

This material is based upon work supported by the National Science Foundation under Grant No. 0910657. We thank Zulma Jiménez for initial help and discussions.

REFERENCES

(1) Scott, S. K.; Showalter, K. Simple and Complex Propagating Reaction−Diffusion Fronts. *J. Phys. Chem.* **1992**, *96*, 8702–8711.

(2) Bánsági, T.; Palczewski, C.; Steinbock, O. Scroll Wave Filaments Terminate in the Back of Traveling Fronts. *J. Phys. Chem. A* **2007**, *111*, 2492–2497.

(3) Orbán, M.; Kurin-Csörgei, K.; Zhabotinsky, A. M.; Epstein, I. R. New Indicators for Visualizing Pattern Formation in Unacatlyzed Bromate Oscillatory Systems. *J. Am. Chem. Soc.* **1998**, *120*, 1146–1150.

(4) Shao, X.; Wu, Y.; Zhang, J.; Wang, H.; Quyang, Q. Inward Propagating Chemical Waves in a Single Reaction−Diffusion System. *Phys. Rev. Lett.* **2008**, *100*, 198304.

(5) Ertl, G. Reactions at Surfaces: From Atoms to Complexity. *Angew. Chem., Int. Ed.* **2008**, *47*, 3524–3535.

(6) Larter, R. Understanding Complexity in Biophysical Chemistry. *J. Phys. Chem. B* **2003**, *107*, 415–429.

(7) Weiss, J. N.; Qu, Z. L.; Chen, P. S.; Lin, S. F.; Karagueuzian, H. S.; Hayashi, H.; Garfinkel, A.; Karma, A. The Dynamics of Cardiac Fibrillation. *Circulation* **2005**, *112*, 1232–1240.

(8) Wellner, M.; Zemlin, C.; Pertsov, A. M. Frustrated Drift of an Anchored Scroll-Wave Filament and the Geodesic Principle. *Phys. Rev. E* **2010**, *82*, 036122.

(9) Jahnke, W.; Skaggs, W. E.; Winfree, A. T. Chemical Vortex Dynamics in the Belousov−Zhabotinsky Reaction and in the Two-Variable Oregonator Model. *J. Phys. Chem.* **1989**, *93*, 740–749.

(10) Barkley, D. Euclidean Symmetry and the Dynamics of Rotating Spiral Waves. *Phys. Rev. Lett.* **1994**, *72*, 164–167.

(11) Keener, J. P.; Tyson, J. J. The Dynamics of Scroll Waves in Excitable Media. *SIAM Rev.* **1992**, *34*, 1–39.

(12) Bánsági, T.; Steinbock, O. Nucleation and Collapse of Scroll Rings in Excitable Media. *Phys. Rev. Lett.* **2006**, *97*, 198301.

(13) Dutta, S.; Steinbock, O. Steady Motion of Hairpin-Shaped Vortex Filaments in Excitable Systems. *Phys. Rev. E* **2010**, *81*, 055202(R).

(14) Sutcliffe, P. M.; Winfree, A. T. Stability of Knots in Excitable Media. *Phys. Rev. E* **2003**, *68*, 016218.

(15) Pertsov, A. M.; Wellner, M.; Vinson, M.; Jalife, J. Topological Constraint on Scroll Wave Pinning. *Phys. Rev. Lett.* **2000**, *84*, 2738–2741.

(16) Jiménez, Z. A.; Marts, B.; Steinbock, O. Pinned Scroll Rings in an Excitable System. *Phys. Rev. Lett.* **2009**, *102*, 244101.

(17) Jiménez, Z. A.; Steinbock, O. Pinning of Vortex Rings and Vortex Networks in Excitable Systems. *Europhys. Lett.* **2010**, *91*, 50002.

(18) Margerit, D.; Barkley, D. Cookbook Asymptotics for Spiral and Scroll Waves in Excitable Systems. *Chaos* **2002**, *12*, 636–649.

(19) Marts, B.; Bánsági, T.; Steinbock, O. Evidence for Burgers' Equation Describing the Untwisting of Scroll Rings. *Europhys. Lett.* **2008**, *83*, 30010.

(20) Cherry, E. M.; Fenton, F. H. Visualization of Spiral and Scroll Waves in Simulated and Experimental Cardiac Tissue. *New J. Phys.* **2008**, *10*, 125016.

(21) Vigmond, E.; Vadakkumpadan, F.; Gurev, V.; Arevalo, H.; Deo, M.; Plank, G.; Trayanova, N. Towards Predictive Modelling of the Electrophysiology of the Heart. *Exp. Physiol.* **2009**, *94*, 563–577.

(22) Barkley, D. Barkley Model. *Scholarpedia* **2008**, *3*, 1877.

(23) Dowle, M.; Mantel, R. M.; Barkley, D. Fast Simulations of Waves in Three-Dimensional Excitable Media. *Int. J. Bifurcation Chaos Appl. Sci. Eng.* **1997**, *7*, 2529–2546.